Fast non-recursive 1D inversion by filtering acoustic reflection data

Evert Slob and Kees Wapenaar, TU Delft; Sven Treitel, Tridekon*

SUMMARY

We derive a fast acoustic inversion method for a piecewise homogeneous horizontally layered medium. The method obtains medium parameters from the reflection response. The method can be implemented to obtain the parameters on either side of a reflector at an arbitrary depth. Three processing steps lead to the inversion result. First, we solve a modified Marchenko type equation to obtain a focusing wavefield. We then apply wavefield continuation across a reflecting boundary to the focusing wavefield and retrieve the reflection coefficient of a reflector as a function of horizontal slowness. Finally, we use the reflection coefficient to obtain the velocities and the ratio of the densities above and below the reflector. Because the two-way traveltime difference of the primary reflection and the one above it becomes known during the process, the thickness of the layer above the reflector is also found. The method can be applied multiple times in different zones, or recursively in a target zone without having to solve more Marchenko type equations. The numerical example illustrates that the method works well on modeled data without the need for a priori model information.

INTRODUCTION

Half a decade ago, a Marchenko scheme was presented that computes vertical seismic profiles (VSP) for a virtual receiver at an arbitrary subsurface location from the measured acoustic reflection response (Broggini & Snieder, 2012; Wapenaar *et al.*, 2013). The required redatuming operators are called focusing functions and are computed from the data when an estimate of the first arrival at the virtual receiver location is available. This scheme was simplified by deriving coupled Marchenko-type equations for the up- and downgoing parts of the focusing wavefields and the VSP. These can be used directly for imaging without artefacts from internal multiples in the data (Slob *et al.*, 2014; Wapenaar *et al.*, 2014). The required velocity model can be the same as used for conventional migration. Implementations that account for free surface and internal multiples exist for land (Singh *et al.*, 2017) and marine (Ravasi, 2017) acoustic data.

Approximately five decades ago, work was done in 1D to understand the relations between up- and downgoing waves from one reflector to the next and recurse through a layered medium given reflection data (Robinson, 1967). These ideas were developed further to carry out inversion using only the reflection response (Robinson & Treitel, 1978). The inversion was carried out in recursive form by moving from the acquisition level down to the bottom reflector, followed by recursively moving back to the acquisition surface while recovering all reflection coefficients. Elements of the formulations used in those works have a striking resemblance to the focusing functions used in th 1D version of Marchenko redatuming and imaging.

Here we combine the idea of recursive inversion presented five decades ago with the non-recursive property of Marchenko redatuming and true amplitude imaging. To stay close to the recursive inversion idea in 1D and facilitate the physical understanding we perform the analysis in 1D. We begin by showing that the reflection response above a layered model can be written as the ratio of two functions as shown by Goupillaud (1961) and we connect them to the up- and downgoing parts of the focusing function. We then show how we can avoid the need for recursion of Robinson & Treitel (1978) by using the Marchenko-type Green's function representations. We follow by showing how wavefield continuation moves the up- and downgoing parts of the focusing functions across a reflecting boundary and how the reflection coefficient can be obtained. We find the velocities and the ratio of densities on either side of the boundary from the reflection coefficient. The inversion ends with computing the layer thickness of the layer just above the reflector for which the refection coefficient is found. We illustrate the method with a numerical example.

OBTAINING LOCAL REFLECTION COEFFICIENTS

We use a horizontally layered medium for simplicity and perform the analysis in the $\tau - p$ domain, with τ being intercept time and p horizontal slowness. This simplification is not necessary, but facilitates the physical understanding of the method. We assume a homogeneous half space in the top, above depth level z_0. The source and receiver are present in the upper half space with $z^s = z^r < z_0$. The lower half space exists for $z > z_m$. There are $m+1$ reflecting boundaries and m layers with finite thickness. In each layer $\mathbb{D}_n$ for $z_{n-1} < z < z_n$ the acoustic velocity is v_n and the density is ρ_n. The horizontal slowness dependent one-way vertical travel time is $t_n = d_n q_n / v_n$ with $q_n = \sqrt{1-(pv_n)^2}$, and with layer thickness $d_n = z_n - z_{n-1}$. The total one-way traveltime to a boundary z_n is given by $\tau_n = (z_0 - z^s)q_0/v_0 + \sum_{k=1}^{n} t_k$. The plane wave reflection response of the layered medium in the frequency domain can be given by (Goupillaud, 1961)

$$\hat{R}_0(p,\omega) = \frac{\hat{f}_1^-(z_0, z_m, p, \omega)}{\hat{f}_1^+(z_0, z_m, p, \omega)}, \tag{1}$$

where the diacritical hat indicates quantities in the frequency domain and we omit ω in the arguments from here onward. The right-hand side is the ratio of the upgoing, $\hat{f}_1^-$, and the downgoing, $\hat{f}_1^+$, parts of the focusing function with the receiver just above the upper reflector at z_0 and the focus point just below the bottom reflector at z_m. Goupillaud gave the expression with slightly different functions. A common factor in the numerator and denominator can be included or excluded without changing the ratio. This can be an amplitude as in the representation of Goupillaud, or a phase as in Robinson & Treitel (1978). If we take $p = 0$ we describe normal incidence plane waves and the expression is the frequency domain equivalent of the expression in Robinson & Treitel (1978) who used z-transforms and discrete time. They showed how one can recurse to the bottom and then back to the top while recovering all primary reflection coefficients. Here we want to

establish two things. We want to be able to start and stop at any depth level while recovering the primary reflection coefficient between those levels, and we want to be able to extend the theory to 3D. In case the medium is 3D, the analysis can be done in the space domain.

Instead of using receivers just below the bottom reflector, we can put them anywhere in the model, e.g., at z_n, and this leads to a Green's function representation given by

$$\hat{R}_0(p)\hat{f}_1^+(z_0,z_n,p) = \hat{f}_1^-(z_0,z_n,p) + \hat{G}^-(z_n,z_0,p), \quad (2)$$

where the Green's function in the right-hand side of equation 2 is the impulse response of the entire layered medium that is upgoing at the receiver at z_n and with a source at z_0. In time reversal we have (Slob *et al.*, 2014)

$$[\hat{R}_0(p)]^*\hat{f}_1^-(z_0,z_n,p) = \hat{f}_1^+(z_0,z_n,p) - [\hat{G}^+(z_n,z_0,p)]^*, \quad (3)$$

where the asterisk in superscript denotes complex conjugation. The Green's function in equation 3 is downgoing at the receiver and overlaps with the direct part of the upgoing focusing function. To keep the focusing functions in the data domain of two-way travel time, we introduce the functions (van der Neut & Wapenaar, 2016)

$$\hat{h}^{\pm}(z_0,z_n,p) = \hat{G}_d^+(z_n,z_0,p)\hat{f}_1^{\pm}(z_0,z_n,p), \quad (4)$$

where $\hat{G}_d^+$ denotes the direct wave from the source at z_0 to the receiver at z_n and

$$\hat{G}_d^+(z_n,z_0,p)\hat{f}_{1d}^+(z_0,z_n,p) = 1, \quad (5)$$

where $\hat{f}_{1d}^+(z_0,z_n,p)$ denotes the direct wave of the downgoing focusing function, which is unknown and needs to be estimated by independent means. The choice of equation 4 removes this unknown. Using equation 4 in equations 2 and 3 gives

$$\hat{R}_0(p)\hat{h}^+(z_0,z_n,p) = \hat{h}^-(z_0,z_n,p) + \hat{U}^-(z_n,z_0,p), \quad (6)$$

$$[\hat{R}_0(p)]^*\hat{h}^-(z_0,z_n,p) = \hat{h}^+(z_0,z_n,p) - [\hat{U}^+(z_n,z_0,p)]^*. \quad (7)$$

These equations have an advantage over the usual Marchenko-type Green's function representations. The new focusing functions, $\hat{h}^{\pm}$ are causal and the reflections occur in the upgoing part at two-way traveltime. The consequence is that the arrival time does not depend on the focusing depth. In equation 6 the modified Green's function is $\hat{U}^-$. Let's have a look at these wavefields in the time domain with a numerical example. We take a medium with three reflectors and two layers which have a thickness of 205 m and 293 m, with velocities of 3000 m/s and 1500 m/s, and densities of 2250 kg/m^3 and 1000 kg/m^3. The source and receiver are located 110 m above the first reflector in a half space with velocity of 1500 m/s and density of 1000 kg/m^3. The lower half space has a velocity of 2000 m/s and density of 1500 kg/m^3. When we analyse the data we do not know depths to interfaces or velocities and only know two-way traveltime as recording time. For that reason we introduce two-way traveltime to any depth level in the layered medium as the new variable ζ. The source emits a Ricker wavelet with 30 Hz center frequency. Figure 1 shows in (a) and (b) the modeled left-hand sides of equations 6 and 7 in the time domain and for $p = 0$. The black solid lines indicate the two-way vertical travel time to the three boundaries. The dashed black lines mark the division between waves that belong to $h^{\pm}$ and that belong to $U^{\pm}$. In Figure 1a the waves that belong to h^- are left of the line and that belong to U^- are right of the line. When a solid line coincides with the dashed line, which occurs at $\tau = \zeta$, the event jumps from U^- to h^-. In Figure 1b the waves that belong to h^+ are right of the line and those that belong to the time-reverse of U^+ are left of the line. At $\tau = 0$ the initial pulse from h^+ coincides with the first event in U^+. From zero time to the first reflector Figure 1a shows the data as recorded because the focusing depth level is still in the upper half space. At $\zeta = 0.147$ s the first reflection moves from U^- to h^-. At $\zeta = 0.283$ s the second reflection moves from U^- to h^-. It changes amplitude because we remove the two-way transmission effects from the primary reflection in the data. The event that belongs to the third primary reflection is then also changed and this becomes the first event in U^-. The two multiples that occur between the second and third primary reflections in the data and in U^- until focusing occurs at the two-way traveltime of 0.283 s are no longer present for deeper focusing levels. When focusing occurs for two-way traveltime of 0.674 s and later, U^- vanishes because we are focusing below the last reflector. At the same time the third primary moves to h^- and receives its correct local reflection strength and a fourth arrival is introduced that is necessary to make U^- equal to zero. This is the reflection from a multiple eliminator.

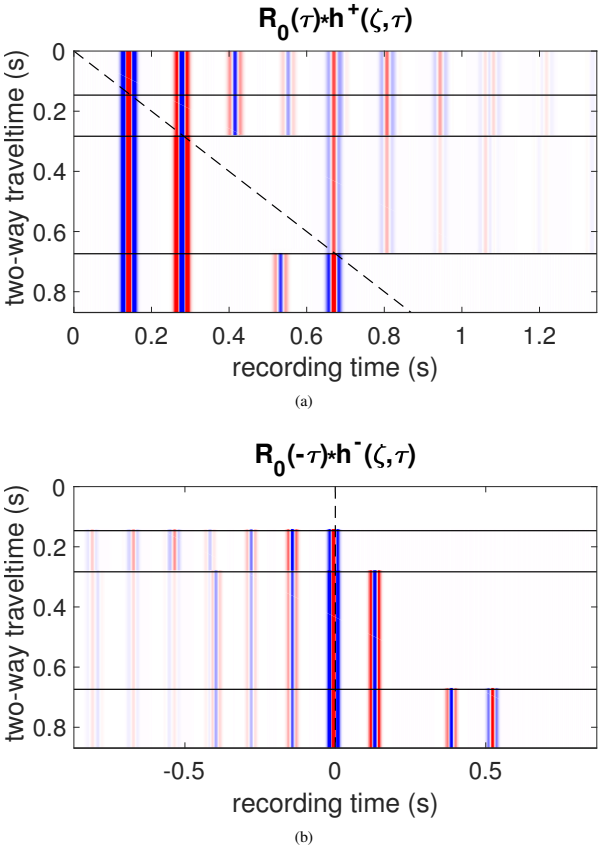

Figure 1: Reflection response (a) convolved with $h^+(z_0,\zeta,\tau)$ and (b) correlated with $h^-(z_0,\zeta,\tau)$, as a function of two-way traveltime ζ and recording time τ.

The example shows we can rely on recording time and two-way traveltime, which are equivalent. Because ζ is equivalent to τ we don't require a velocity model to compute the wavefields $h^{\pm}$ and $U^{\pm}$. It has the advantage that we keep the results in the same coordinate system as the data. In the time domain we can apply a time window and write the modified Marchenko equations as

$$h^-(z_0,z_n,\tau,p) = \int_{t'=0}^{\tau} h^+(z_0,z_n,\tau-t',p)R(t',p)\mathrm{d}t', \quad (8)$$

$$h_m^+(z_0,z_n,\tau,p) = \int_{t'=0}^{\tau} h^-(z_0,z_n,\tau+t',p)R(t',p)\mathrm{d}t', \quad (9)$$

$$h^+(z_0,z_n,\tau,p) = \delta(\tau)+h_m^+(z_0,z_n,\tau,p), \quad (10)$$

which are valid for $\tau < 2\tau_n(p)$ and we have used $h_m^+(z_0,z_n,\tau,p)$ to denote the emitted waves that follow the initial impulse. These modified focusing functions allow for making the connection to Robinson (1967) who showed that a recursion relation exists between the up- and downgoing parts of modified focusing functions. For the focusing functions we use here these recursion relations are given by

$$\hat{h}^{\pm}(z_0,z_n,p) = \hat{h}^{\pm}(z_0,z_{n-1},p) + r_n(p)\exp(-2\mathrm{i}\omega\tau_n)[\hat{h}^{\mp}(z_0,z_{n-1},p)]^*. \quad (11)$$

For $p=0$ and formulated in z-transforms, equation 11 would be similar to equation 3.2 in Robinson & Treitel (1978). Notice that these relations remain valid for any pair of depth levels on either side of a single reflector and depend only on the two-way traveltime between acquisition level and the reflector. Equation 11 avoids solving the Marchenko equations more than once. Suppose we solve the coupled equations 8 and 9 to some distance above the target level, e.g., to depth level $z_\alpha < z_j$ with z_j the depth of the jth reflector. The corresponding two-way traveltime is $\zeta_\alpha < \zeta_j$. We then know $h^{\pm}(z_0,\zeta_\alpha,\tau,p)$, evaluate equation 8 at ζ_β with $\zeta_j < \zeta_\beta < \zeta_{j+1}$ and use equation 11 to find the reflection coefficient as

$$r_j(p) = \frac{U^-(z_0,\zeta_\alpha,2\tau_j,p)}{U^+(z_0,\zeta_\alpha,0,p)}, \quad (12)$$

which result is known (Slob *et al.*, 2014; Wapenaar *et al.*, 2014). In 1D $U^+(z_0,\zeta,0,p)=1$ for any focusing depth with two-way traveltime ζ and the division can be omitted. In 3D a linear integral equation must be solved. The interesting point here is that this result can be used to obtain the focusing functions below the reflector at z_j without solving a new set of Marchenko equations. From the functions $h^{\pm}(z_0,\zeta_\alpha,\tau,p)$ the reflection coefficient r_j can be computed from equation 12. Then $h^{\pm}(z_0,\zeta_\beta,\tau,p)$ can be computed using $h^{\pm}(z_0,\zeta_\alpha,\tau,p)$ and r_j in equation 11 and r_{j+1} can be found by repeating the procedure. In that case it becomes a recursive scheme.

OBTAINING LAYER VELOCITIES, DENSITY RATIO, AND LAYER THICKNESS

Let us assume we have computed $r_j(p)$ using equation 12 for several p-values. The reflection coefficient is given by

$$r_j(p) = \frac{\rho_{j+1}v_{j+1}q_j - \rho_j v_j q_{j+1}}{\rho_{j+1}v_{j+1}q_j + \rho_j v_j q_{j+1}}, \quad (13)$$

in which q_n is defined above equation 1. The impedance ratio is obtained from $r_j(0)$ as

$$\beta = \frac{\rho_{j+1}v_{j+1}}{\rho_j v_j} = \frac{1+r_j(0)}{1-r_j(0)}, \quad (14)$$

and we can define the ratio of the squared q-factors as

$$\alpha(p) = \frac{1-(pv_{j+1})^2}{1-(pv_j)^2} = \beta^2\left(\frac{1-r_j(p)}{1+r_j(p)}\right)^2. \quad (15)$$

Suppose the ray parameter is sampled with $K+1$ samples as p_k with $k=0,1,2,\cdots,K$ and $p_0=0$. We then find the velocities on either side of the boundary from the 2×2 equation

$$\sum_{l=1}^{2} \mathsf{A}_{il}c_l = b_i, \quad (16)$$

with $i=1,2$, $c_1=(v_{j+1}/v_0)^2$, $c_2=(v_j/v_0)^2$ and

$$A_{il} = \frac{1}{K}\sum_{k=1}^{K}[-\alpha(p_k)]^{(i+l-2)}, \quad (17)$$

$$b_i = \frac{1}{K}\sum_{k=1}^{K}\frac{[-\alpha(p_k)]^{i-1}[1-\alpha(p_k)]}{(v_0p_k)^2}. \quad (18)$$

The velocities can be computed as

$$v_j = \sqrt{c_2}v_0, \qquad v_{j+1} = \sqrt{c_1}v_0. \quad (19)$$

The last step is to compute the density ratio from

$$\frac{\rho_{j+1}}{\rho_j} = \beta\frac{v_j}{v_{j+1}}. \quad (20)$$

The two-way travel time of the last event in $h^{\pm}(z_0,\zeta_\alpha,\tau,0)$ is equal to $2\tau_{j-1}$ and to compute r_j we have used $2\tau_j$. We can compute the layer thickness as

$$d_j = (\tau_j-\tau_{j-1})v_j. \quad (21)$$

With this result the inversion is complete.

NUMERICAL EXAMPLE

We illustrate our scheme with a model with 11 reflectors. The layer properties in the model are given in Table 1. Figure 2 shows the first 3.3 s of the recorded reflection response with a 30 Hz center frequency Ricker wavelet as source signal. It can be observed from Figure 2 that the multiples obscure the primaries from approximately 2 s onwards. We can assume the relatively high amplitude event at 1.86 s is a primary reflection and we choose to solve the Marchenko equations 8 and 9 for $\zeta = 1.9$ s. Figure 3 shows a zoomed version at three values of ζ from 1.6 s to 2.6 s. The first is a zoomed trace in green colour and it is equal to the data. The second trace is $h^-(z_0,\zeta=1.9,\tau,0)+U^-(z_0,\zeta=1.9,\tau,0)$ where the part of h^- is black and the part of U^- is green. The two-way traveltime of $\zeta=1.9$ s is after the 6th but before the 7th primary reflection has occurred. The third trace is $h^-(z_0,\zeta=2.1,\tau,0)+U^-(z_0,\zeta=2.1,\tau,0)$ where the part of h^- is black and the part of U^- is green. The two-way traveltime of $\zeta=2.1$ s is after the 7th but

Table 1: Values for velocity, density, and layer thickness in the layered model.

layer number	velocity (m/s)	density (kg/m^3)	thickness (m)
1	1700	1430	∞
2	2300	2750	151
3	1900	2000	184
4	1700	1430	307
5	2100	1750	433
6	3200	2930	672
7	2000	1750	98
8	2100	2110	310
9	3300	1970	197
10	2500	2110	398
11	2750	2250	325
12	2900	2300	∞

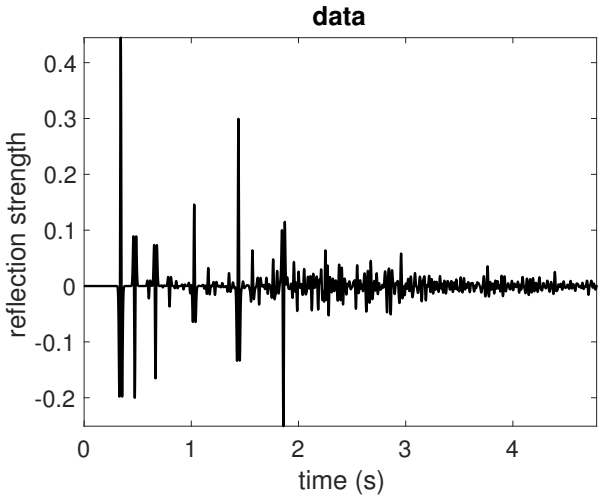

Figure 2: Reflection response to vertical incident plane wave and receiver 290 m above first reflector.

before the 8^{th} primary reflection has occurred. All three traces have the same scaling and display true amplitudes.

The trace in the middle of Figure 3 is computed by solving equations 8 and 9 for $\zeta_\alpha = 1.9$ s and h^- is the black part of the trace. Then U^- is computed from equation 6 and it is the green part of the trace. The last reflector in black in the middle trace is the reflection of the 6^{th} reflector. Moving the focusing level down to 1.9 s two-way traveltime has increased its amplitude compared with its amplitude in the data. Moving the event to h^- has removed overlapping multiple reflections and removed the transmission effects. The primary reflection of the 7^{th} reflector cannot be distinguished from the multiples in the data, shown in the top trace in green. It has become visible in the trace in the middle as the first event in the green part. This is part of U^- and this means it must be a primary reflection. Assuming it is a reflector of interest we first find its reflection coefficient from equation 12. We then compute $h^\pm(z_0,\zeta_\beta,\tau,p)$ with equation 11 and compute $U^-(z_0,\zeta_\beta,\tau,p)$ from equation 6 and display them as the third trace in Figure 3.

We choose $\zeta_\beta = 2.1$ s as indicated in the bottom trace. The first green event in the middle trace has become a black event with increased amplitude as the last event of h^-. We emphasize that the strength of this reflector is obtained without computing the bottom trace, which is possible with the aid of equation 12 and the knowledge of $h^\pm(z_0,\zeta_\alpha = 1.9,\tau,0)$ and the reflection data.

We compute the reflection coefficient r_7 for 10 p-values corresponding to incidence angles ranging from 0^o to 30^o, which amounts to the range 0^o to 36^o locally. From these 10 values we obtain the velocities of 2000 m/s and 2100 m/s in layers 7 and 8 and density ratio 1.21 and a computed layer thickness of 98 m with errors less than 0.1%. Of course, this is an optimal example with noise free data and complete knowledge of the source signature. What we show here is that the method works in theory. We believe it is of interest that no model information is required to perform non-recursive inversion of one reflection event at a two-way traveltime of choice.

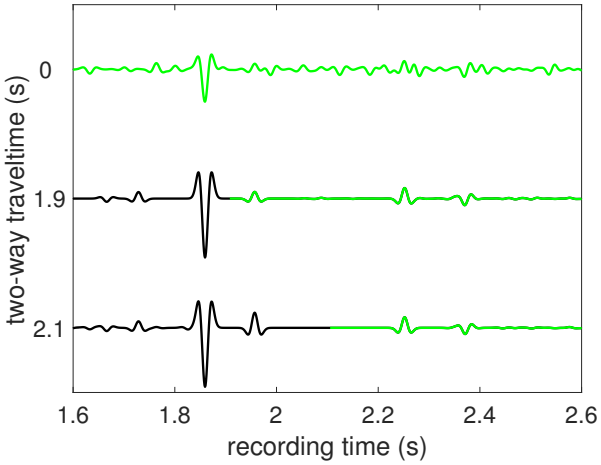

Figure 3: Zoomed part of the data in green at zero vertical two-way travel time, h^- in black and U^- in green at two-way traveltimes before and after that of the 7^{th} reflector.

CONCLUSIONS

We have connected the theory of Marchenko redatuming with the theory of recursive wavefield continuation across a reflecting boundary. This combination allows for non-recursive inversion. Because we start the focusing function always as a unit impulse at zero time, the scheme does not use model information. As a consequence the modified Marchenko equation is not solved for a particular depth, but for traveltime. The scheme requires solving the Marchenko equations for a chosen two-way traveltime. Then the reflection coefficient is computed of the first reflection that arrives after the chosen time. From the reflection coefficient the wave velocity on either side of the reflector is obtained with the ratio of the densities and the thickness of the layer just above the reflector. The absolute depth of the reflector remains unknown unless the whole medium is inverted for. If the method is recursively applied from a target depth level onwards, the Marchenko equation is solved only once. Numerical implementation in 2D and 3D, robustness in case of noise, and practical implementation remain to be investigated.

REFERENCES

Broggini, F., & Snieder, R. 2012. Connection of scattering principles: a visual and mathematical tour. *European Journal of Physics*, **33**(3), 593–613.

Goupillaud, P. L. 1961. An approach to inverse filtering of near surface effects from seismic records. *Geophysics*, **26**, 754–760.

Ravasi, M. 2017. Rayleigh-Marchenko redatuming for target-oriented, true-amplitude imaging. *Geophysics*, **82**(6), S439–S452.

Robinson, E. A. 1967. *Multichannel time series analysis with digital computer programs*. San Francisco: Holden-Day Inc.

Robinson, E. A., & Treitel, S. 1978. Fine-structure of normal incidence synthetic seismogram. *Geophysical Journal of the Royal Astronomical Society*, **53**, 289–309.

Singh, S., Snieder, R., van der Neut, J., Thorbecke, J., Slob, E. C., & Wapenaar, K. 2017. Accounting for free-surface multiples in Marchenko imaging. *Geophysics*, **82**(1), R19–R30.

Slob, E., Wapenaar, K., Broggini, F., & Snieder, R. 2014. Seismic reflector imaging using internal multiples with Marchenko-type equations. *Geophysics*, **79**(2), S63–S76.

van der Neut, J., & Wapenaar, K. 2016. Adaptive overburden elimination with the multidimensional Marchenko equation. *Geophysics*, **81**(5), T265–T284.

Wapenaar, K., Broggini, F., Slob, E., & Snieder, R. 2013. Three-Dimensional Single-Sided Marchenko Inverse Scattering, Data-Driven Focusing, Green's Function Retrieval, and their Mutual Relations. *Physical Review Letters*, **110**(8), 084301.

Wapenaar, K., Thorbecke, J., van der Neut, J., Broggini, F., Slob, E., & Snieder, R. 2014. Marchenko Imaging. *Geophysics*, **79**(3), WA39–WA57.